# FSI and reduced models for 3D hemodynamic simulations in time-dependent domains

Yuri Vassilevski[1,2,3]

[1]Marchuk Institute of Numerical Mathematics RAS
[2]Moscow Institute of Physics and Technology
[3]Sechenov University

*The 8th European Congress of Mathematics*

*Multiscale Modeling and Methods: Application in Engineering, Biology and Medicine*

June 22, 2021

The work was supported by the Russian Science Foundation

# Related talks and minisymposia

- Monday, PL: Alfio Quarteroni (Politecnico di Milano and EPFL), *The beat of math*
- Tuesday,Wednesday, MS80: *Multiscale modeling and methods: application in engineering, biology and medicine*
- Tuesday,Wednesday, MS36: *Mathematical analysis: the interaction of fluids/ viscoelastic materials and solids*
- Thursday,Friday, MS35: *Mathematics in biology and medicine*

# Joint work with

- Maxim Olshanskii, University of Houston
- Alexander Danilov, INM RAS, Sechenov University
- Alexander Lozovskiy, INM RAS
- Victoria Salamatova, Sechenov University
- Tatiana Dobroserdova, INM RAS
- Grigory Panassenko, University Jean Monnet
- Alexei Lyogkii, MIPT

# Fluid-Structure Interaction problem

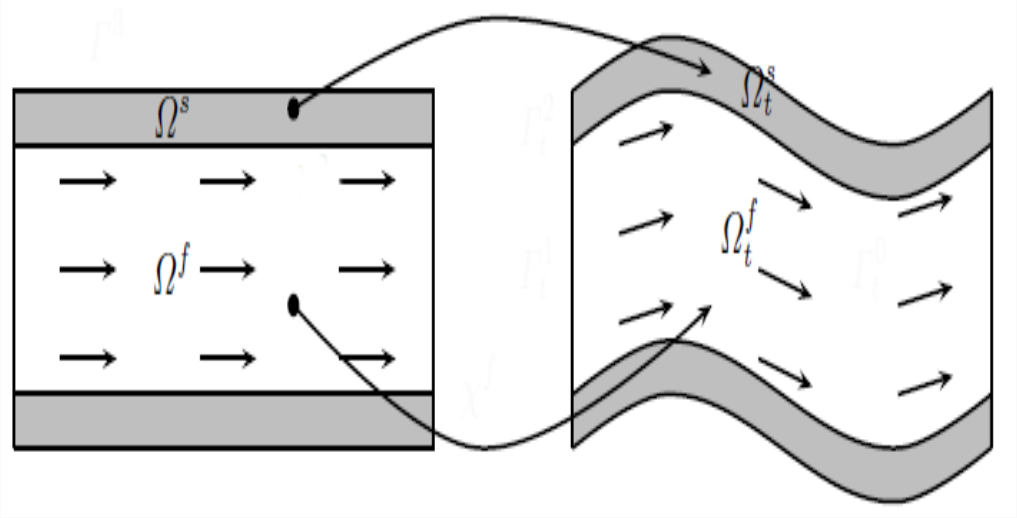


- reference subdomains $\Omega_f$, $\Omega_s$
- transformation $\boldsymbol{\xi}$ maps $\Omega_f$, $\Omega_s$ to $\Omega_f(t)$, $\Omega_s(t)$
- $\mathsf{v}$ and $\mathsf{u}$ denote velocities and displacements in $\widehat{\Omega} := \Omega_f \cup \Omega_s$
- $\boldsymbol{\xi}(\mathsf{x}) := \mathsf{x} + \mathsf{u}(\mathsf{x})$, $\mathsf{F} := \nabla\boldsymbol{\xi} = \mathsf{I} + \nabla\mathsf{u}$, $J := \det(\mathsf{F})$
- Cauchy stress tensors $\boldsymbol{\sigma}_f$, $\boldsymbol{\sigma}_s$
- pressures $p_f$,$p_s$
- density $\rho_f$ is constant

# Fluid-Structure Interaction problem

Dynamic equations

$$\frac{\partial \mathbf{v}}{\partial t} = \begin{cases} \rho_s^{-1}\mathrm{div}\,(J\boldsymbol{\sigma}_s\mathbf{F}^{-T}) & \text{in } \Omega_s, \\ (J\rho_f)^{-1}\mathrm{div}\,(J\boldsymbol{\sigma}_f\mathbf{F}^{-T}) - \nabla\mathbf{v}\left(\mathbf{F}^{-1}\left(\mathbf{v} - \dfrac{\partial \mathbf{u}}{\partial t}\right)\right) & \text{in } \Omega_f \end{cases}$$

Kinematic equation

$$\frac{\partial \mathbf{u}}{\partial t} = \mathbf{v} \quad \text{in } \Omega_s$$

Fluid incompressibility

$$\mathrm{div}\,(J\mathbf{F}^{-1}\mathbf{v}) = 0 \quad \text{in } \Omega_f \quad \text{or} \quad J\nabla\mathbf{v} : \mathbf{F}^{-T} = 0 \quad \text{in } \Omega_f$$

Constitutive relation for the fluid stress tensor

$$\boldsymbol{\sigma}_f = -p_f\mathbf{I} + \mu_f((\nabla\mathbf{v})\mathbf{F}^{-1} + \mathbf{F}^{-T}(\nabla\mathbf{v})^T) \quad \text{in } \Omega_f$$

# FSI problem

Constitutive relation for the solid stress tensor

$$\boldsymbol{\sigma}_s = \boldsymbol{\sigma}_s(J, \mathsf{F}, p_s, \lambda_s, \mu_s, \dots) \quad \text{in } \Omega_s$$

Monolithic approach [1] : Extension of the displacement field to the fluid domain

$$\begin{aligned} G(\mathsf{u}) &= 0 \quad \text{in } \Omega_f, \\ \mathsf{u} &= \mathsf{u}^* \quad \text{on } \partial\Omega_f \end{aligned}$$

for example, vector Laplace equation or elasticity equation

+ Initial, boundary, interface conditions ($\boldsymbol{\sigma}_f \mathsf{F}^{-T} \mathsf{n} = \boldsymbol{\sigma}_s \mathsf{F}^{-T} \mathsf{n}$)

[1] Michler et al (2004), Hubner et al (2004), Hron&Turek (2006),...

# Numerical scheme

- Consistent triangular or tetrahedral mesh $\Omega_h$ in $\widehat{\Omega}$
- LBB-stable pair for velocity and pressure $P_2/P_1$, $P_2$ for displacements
- Open source software `Ani2D`, `Ani3D` (Advanced numerical instruments 2D/3D, K.Lipnikov, Yu.Vassilevski et al.)

  `http://sf.net/p/ani2d/` `http://sf.net/p/ani3d/`:

  - mesh generation
  - FEM systems
  - algebraic solvers

# Numerical scheme

Find $\{\mathbf{u}^{k+1}, \mathbf{v}^{k+1}, p^{k+1}\} \in \mathbb{V}_h^0 \times \mathbb{V}_h \times \mathbb{Q}_h$ satisfying b.c. and $\left[\frac{\partial \mathbf{u}}{\partial t}\right]_{k+1} = \mathbf{v}^{k+1}$ on $\Gamma_{fs}$

$$\int_{\Omega_s} \rho_s \left[\frac{\partial \mathbf{v}}{\partial t}\right]_{k+1} \boldsymbol{\psi} \, \mathrm{d}\Omega + \int_{\Omega_s} J_k \mathbf{F}(\widetilde{\mathbf{u}}^k) \mathbf{S}(\mathbf{u}^{k+1}, \widetilde{\mathbf{u}}^k) : \nabla \boldsymbol{\psi} \, \mathrm{d}\Omega +$$

$$\int_{\Omega_f} \rho_f J_k \left[\frac{\partial \mathbf{v}}{\partial t}\right]_{k+1} \boldsymbol{\psi} \, \mathrm{d}\Omega + \int_{\Omega_f} \rho_f J_k \nabla \mathbf{v}^{k+1} \mathbf{F}^{-1}(\widetilde{\mathbf{u}}^k) \left( \widetilde{\mathbf{v}^k} - \widetilde{\left[\frac{\partial \mathbf{u}}{\partial t}\right]_k} \right) \boldsymbol{\psi} \, \mathrm{d}\Omega +$$

$$\int_{\Omega_f} 2\mu_f J_k \mathbf{D}_{\widetilde{\mathbf{u}}^k} \mathbf{v}^{k+1} : \mathbf{D}_{\widetilde{\mathbf{u}}^k} \boldsymbol{\psi} \, \mathrm{d}\Omega - \int_{\Omega_f} p^{k+1} J_k \mathbf{F}^{-T}(\widetilde{\mathbf{u}}^k) : \nabla \boldsymbol{\psi} \, \mathrm{d}\Omega = 0 \quad \forall \boldsymbol{\psi} \in \mathbb{V}_h^0$$

$$\int_{\Omega_s} \left[\frac{\partial \mathbf{u}}{\partial t}\right]_{k+1} \boldsymbol{\phi} \, \mathrm{d}\Omega - \int_{\Omega_s} \mathbf{v}^{k+1} \boldsymbol{\phi} \, \mathrm{d}\Omega + \int_{\Omega_f} G(\mathbf{u}^{k+1}) \boldsymbol{\phi} \, \mathrm{d}\Omega = 0 \quad \forall \boldsymbol{\phi} \in \mathbb{V}_h^{00}$$

$$\int_{\Omega_f} J_k \nabla \mathbf{v}^{k+1} : \mathbf{F}^{-T}(\widetilde{\mathbf{u}}^k) q \, \mathrm{d}\Omega = 0 \quad \forall \, q \in \mathbb{Q}_h$$

$$J_k := J(\widetilde{\mathbf{u}}^k), \quad \widetilde{\mathbf{f}}^k := 2\mathbf{f}^k - \mathbf{f}^{k-1}, \quad \mathbf{D}_{\mathbf{u}}\mathbf{v} := \{\nabla \mathbf{v} \mathbf{F}^{-1}(\mathbf{u})\}_s, \quad \{\mathbf{A}\}_s := \frac{1}{2}(\mathbf{A} + \mathbf{A}^T)$$

# Numerical scheme

$$\ldots + \int_{\Omega_s} J_k \mathsf{F}(\widetilde{\mathsf{u}}^k)\mathsf{S}(\mathsf{u}^{k+1}, \widetilde{\mathsf{u}}^k) : \nabla \boldsymbol{\psi} \, \mathrm{d}\Omega + \ldots$$

- St. Venant–Kirchhoff model (geometrically nonlinear):

$$\mathsf{S}(\mathsf{u}_1, \mathsf{u}_2) = \lambda_s \mathtt{tr}(\mathsf{E}(\mathsf{u}_1, \mathsf{u}_2))\mathsf{I} + 2\mu_s \mathsf{E}(\mathsf{u}_1, \mathsf{u}_2);$$
$$\mathsf{E}(\mathsf{u}_1, \mathsf{u}_2) = \{\mathsf{F}(\mathsf{u}_1)^T \mathsf{F}(\mathsf{u}_2) - \mathsf{I}\}_s$$

- inc. Blatz–Ko model:

$$\mathsf{S}(\mathsf{u}_1, \mathsf{u}_2) = \mu_s(\mathtt{tr}(\{\mathsf{F}(\mathsf{u}_1)^T \mathsf{F}(\mathsf{u}_2)\}_s)\mathsf{I} - \{\mathsf{F}(\mathsf{u}_1)^T \mathsf{F}(\mathsf{u}_2)\}_s)$$

- inc. Neo-Hookean model:

$$\mathsf{S}(\mathsf{u}_1, \mathsf{u}_2) = \mu_s \mathsf{I}; \; \mathsf{F}(\widetilde{\mathsf{u}}^k) \to \mathsf{F}(\mathsf{u}^{k+1})$$

$$\{\mathsf{A}\}_s := \tfrac{1}{2}(\mathsf{A} + \mathsf{A}^T)$$

# Numerical scheme

The scheme

- provides strong coupling on interface
- semi-implicit
- produces one linear system per time step
- may be first or second order in time
- unconditionally stable (stability estimate without CFL restriction), proved with assumptions:
  - 1st order in time
  - St. Venant–Kirchhoff inc./comp. (experiment: Neo-Hookean inc./comp.)
  - extension of $\mathbf{u}$ to $\Omega_f$ guarantees $J_k > 0$
  - $\Delta t$ is not large

A.Lozovskiy, M.Olshanskii, V.Salamatova, Yu.Vassilevski. An unconditionally stable semi-implicit FSI finite element method. *Comput.Methods Appl.Mech.Engrg., 297, 2015*

# 3D: pressure wave in flexible tube

L.Formaggia et al., *CMAME* 191: 561–582, 2001

$t = 0.004$s

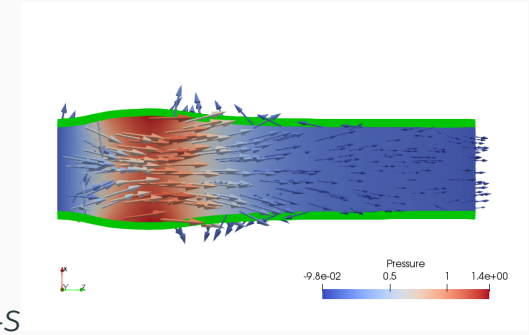


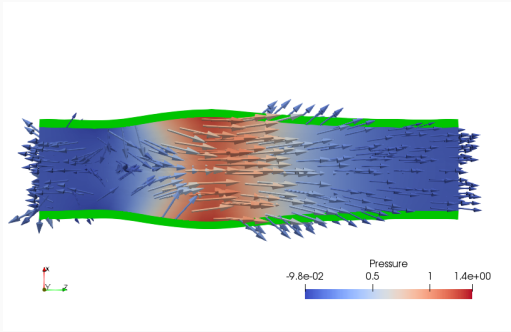


$t = 0.006$s

$t = 0.008$s

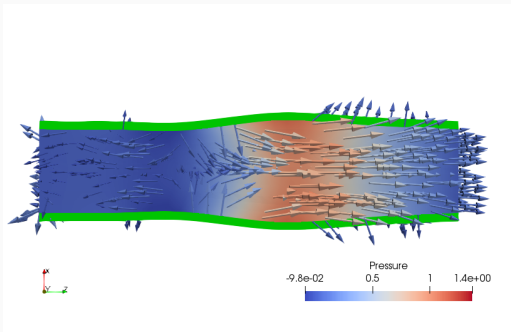


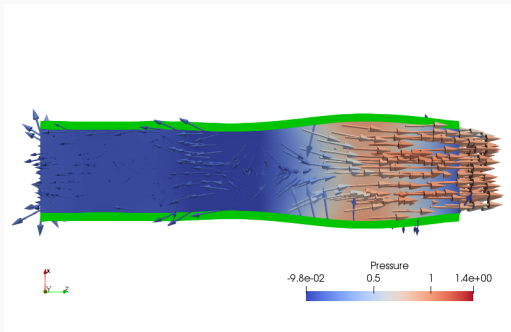


$t = 0.01$s

Pressure wave: middle cross-section velocity field, pressure distribution, velocity vectors and 10× enlarged structure displacement for several time instances

- The tube (fixed at both ends) is 50mm long, it has inner diameter of 10mm and the wall (SVK) is 1mm thick.
- Left end: external pressure $p_{ext}$ is set to $1.333 \cdot 10^3$Pa for $t \in (0, 3 \cdot 10^{-3})$s and zero afterwards, $\boldsymbol{\sigma}_f \mathbf{F}^{-T} \mathbf{n} = p_{ext} \mathbf{n}$. Right end: open boundary
- Simulation was run with $\Delta t = 10^{-4}$ s
- $\#Tets(\Omega_s) = 6336/11904/38016$, $\#Tets(\Omega_f) = 13200/29202/89232$

# 3D: pressure wave in flexible tube

L.Formaggia et al., *CMAME* 191: 561–582, 2001

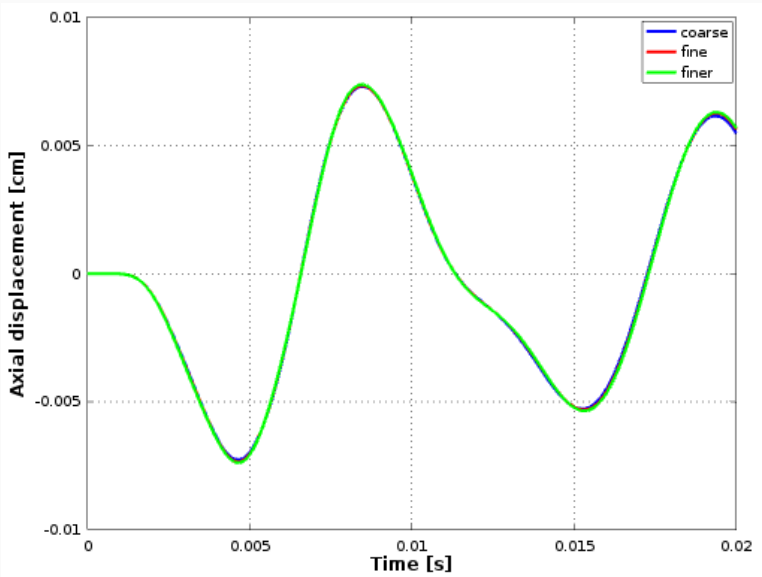


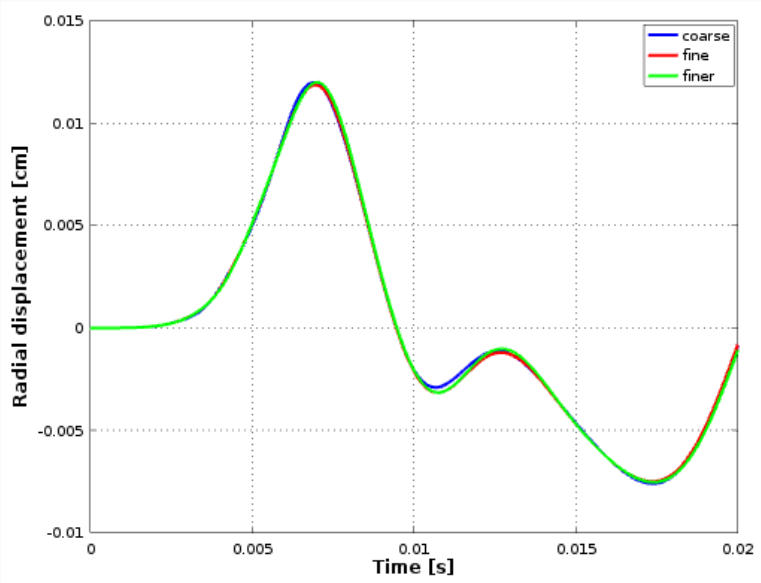


axial component radial component

Pressure wave: The radial and axial components of displacement of the inner tube wall at half the length of the pipe. Solutions are shown for three sequentially refined meshes. The plots are almost indistinguishable.

# 3D: silicone filament in glycerol

Benchmark challenge for CMBE 2015, Paris

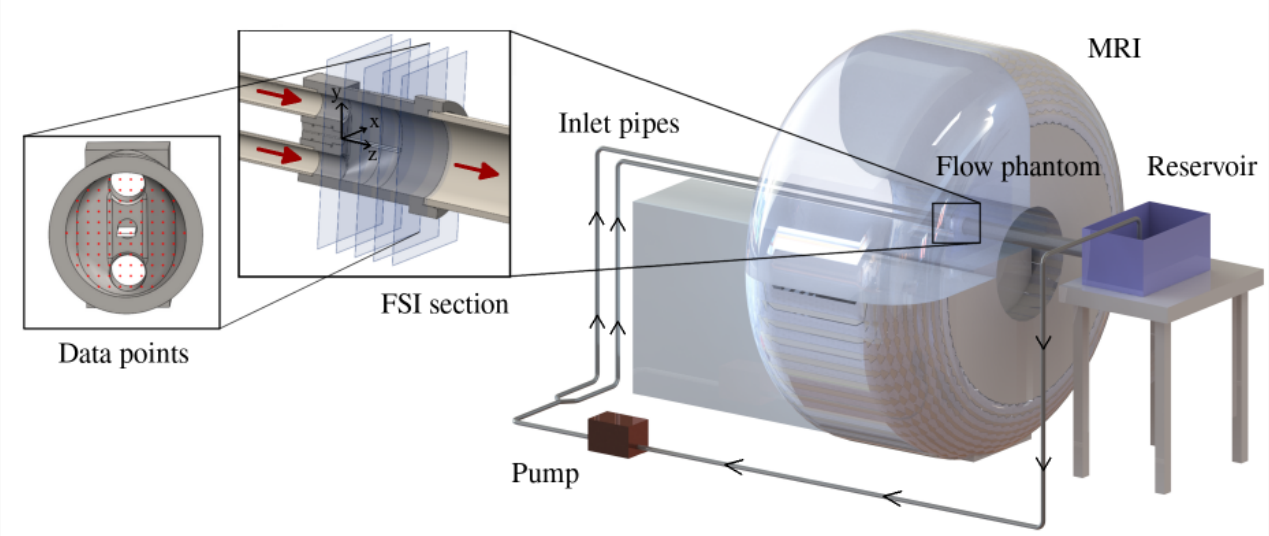


Image from A. Hessenthaler et al. Experiment for validation of fluid-structure interaction models and algorithms. *Int. J. for Numer. Meth. Biomed. Engng.*, 2017

# 3D: silicone filament in glycerol

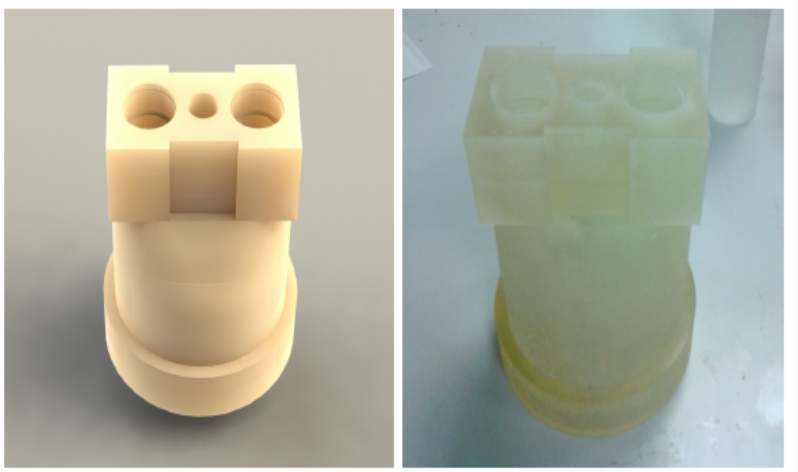

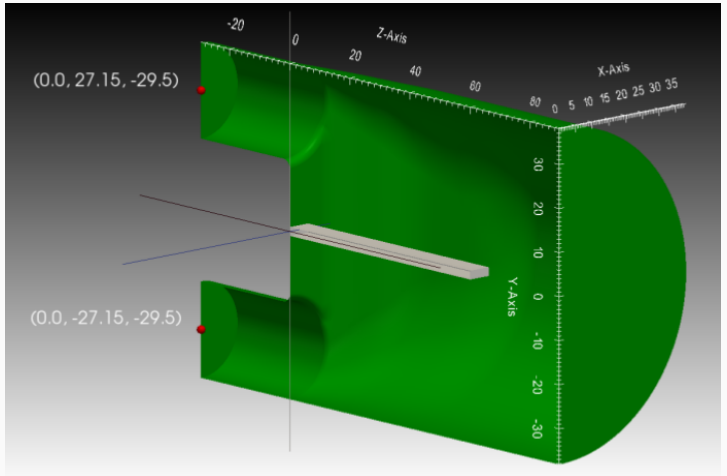


Meshed volume: original and extended domains.

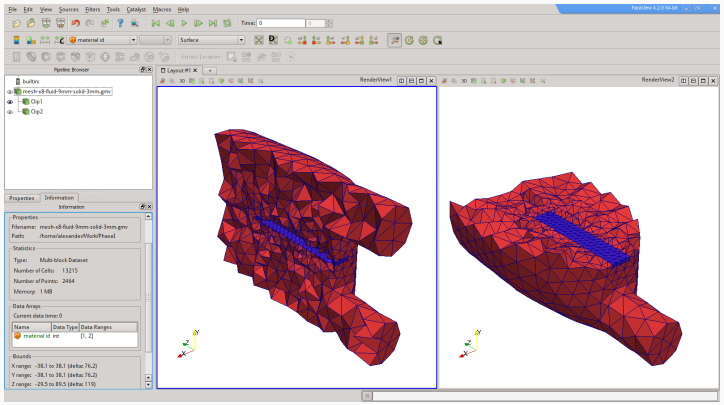

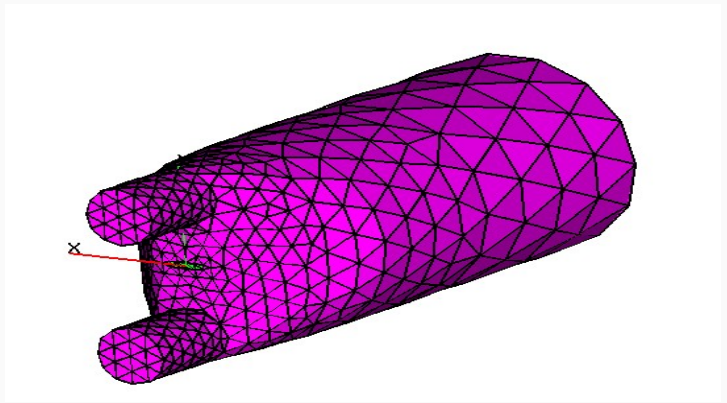

# 3D: silicone filament in glycerol

- Steady and pulsatile flow regimes
- Simulation was run with $\Delta t = 10^{-2}$ s, $t \in [0, 12]$
- $\#Tets(\Omega_s) = 733$, $\#Tets(\Omega_f) = 28712$, $\#unknowns = 254439$
- The filament (SVK) is lighter than the fluid and deflects upward
- Linear elasticity model is used for the **update**[2] of the displacement extension in $\Omega_f$, the Lame parameters are element-volume dependent

[2] M.Landajuela et al. Coupling schemes for the FSI forward prediction challenge: comparative study and validation. *Int. J. for Numer. Meth. in Biomed. Engng.*, 33, 2017.

# 3D: silicone filament in glycerol

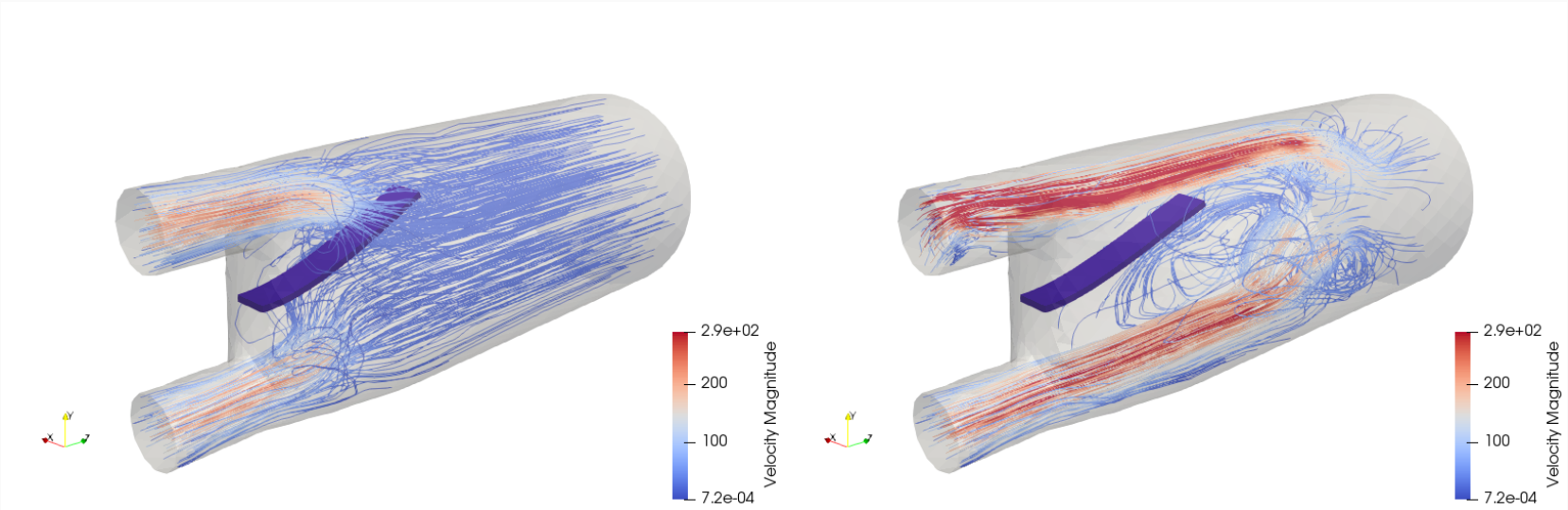


Streamlines colored by the velocity magnitude $t = 0.721$s (left), $t = 2.017$s (right)

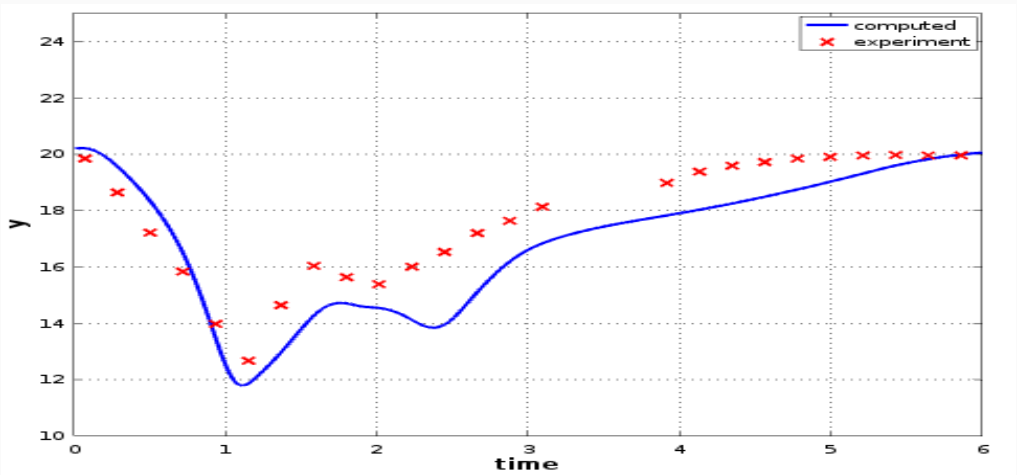


Track of the computed $y$-displacement of the point in the structure with coordinate $z \approx 53$, $x = 0$ for $t \in [0, 6]$ and recorded experimental data



A.Lozovskiy, M.Olshanskii, Yu.Vassilevski. Analysis and assessment of a monolithic FSI finite element method. Computers & Fluids, 179, 2019

# Fluid-structure interaction: pros and cons

Pros:

- FSI is the accurate model providing 3D fields of $p, \mathbf{v}$ in fluid, $\mathbf{u}, \boldsymbol{\sigma}_s$ in structure
- Unconditionally stable semi-implicit FE scheme for FSI is proposed
- Only one linear system is solved per time step
- The scheme can incorporate diverse elasticity models
- Works robustly in 2D and 3D and handles relatively large time steps

# Fluid-structure interaction: pros and cons

Cons:

- FSI is computationally expensive (hours of computation on a parallel cluster with $\sim$ 100 cores )
- Long simulation is not relevant to clinical practice
- Unknown elastic properties of structure
- Boundary conditions for fluid are speculative

# Fluid-structure interaction: pros and cons

Cons:

- FSI is computationally expensive (hours of computation on a parallel cluster with $\sim$ 100 cores )
- Long simulation is not relevant to clinical practice
- Unknown elastic properties of structure
- Boundary conditions for fluid are speculative

Simpler models?

# Example 1

# Incompressible fluid flow in a moving domain

Let $\boldsymbol{\xi}$ mapping $\Omega_0$ to $\Omega(t)$, $\mathsf{F} = \nabla\boldsymbol{\xi} = \mathsf{I} + \nabla\mathsf{u}$, $J = \det(\mathsf{F})$ be given

Dynamic equations

$$\frac{\partial \mathsf{v}}{\partial t} = (J\rho_f)^{-1}\mathrm{div}\,(J\boldsymbol{\sigma}_f\mathsf{F}^{-T}) - \nabla\mathsf{v}\left(\mathsf{F}^{-1}\left(\mathsf{v} - \frac{\partial \mathsf{u}}{\partial t}\right)\right) \quad \text{in } \Omega_0$$

Fluid incompressibility

$$\mathrm{div}\,(J\mathsf{F}^{-1}\mathsf{v}) = 0 \quad \text{in } \Omega_0 \quad \text{or} \quad J\nabla\mathsf{v} : \mathsf{F}^{-T} = 0 \quad \text{in } \Omega_0$$

Constitutive relation for the fluid stress tensor

$$\boldsymbol{\sigma}_f = -p_f\mathsf{I} + \mu_f((\nabla\mathsf{v})\mathsf{F}^{-1} + \mathsf{F}^{-T}(\nabla\mathsf{v})^T) \quad \text{in } \Omega_0$$

Mapping $\boldsymbol{\xi}$ does not define material trajectories $\rightarrow$ quasi-Lagrangian formulation

# Finite element scheme

Let $\mathbb{V}_h, \mathbb{Q}_h$ be Taylor-Hood $P_2/P_1$ finite element spaces.

Find $\{\mathbf{v}_h^k, p_h^k\} \in \mathbb{V}_h \times \mathbb{Q}_h$ satisfying b.c.

("do nothing" $\boldsymbol{\sigma}\mathbf{F}^{-T}\mathbf{n} = 0$ or no-penetration no-slip $\mathbf{v}^k = (\boldsymbol{\xi}^k - \boldsymbol{\xi}^{k-1})/\Delta t$)

$$\int_{\Omega_0} J_k \frac{\mathbf{v}_h^k - \mathbf{v}_h^{k-1}}{\Delta t} \cdot \boldsymbol{\psi} \,\mathrm{d}\mathbf{x} + \int_{\Omega_0} J_k \nabla \mathbf{v}_h^k \mathbf{F}_k^{-1} \left( \mathbf{v}_h^{k-1} - \frac{\boldsymbol{\xi}^k - \boldsymbol{\xi}^{k-1}}{\Delta t} \right) \cdot \boldsymbol{\psi} \,\mathrm{d}\mathbf{x} -$$
$$\int_{\Omega_0} J_k p_h^k \mathbf{F}_k^{-T} : \nabla \boldsymbol{\psi} \,\mathrm{d}\mathbf{x} + \int_{\Omega_0} J_k q \mathbf{F}_k^{-T} : \nabla \mathbf{v}_h^k \,\mathrm{d}\mathbf{x} +$$
$$\int_{\Omega_0} \nu J_k (\nabla \mathbf{v}_h^k \mathbf{F}_k^{-1} \mathbf{F}_k^{-T} + \mathbf{F}_k^{-T} (\nabla \mathbf{v}_h^k)^T \mathbf{F}_k^{-T}) : \nabla \boldsymbol{\psi} \,\mathrm{d}\mathbf{x} = 0$$

$$\int_{\Omega_0} J_k \nabla \mathbf{v}^k : \mathbf{F}_k^{-T} q \,\mathrm{d}\Omega = 0$$

for all $\boldsymbol{\psi}$ and $q$ from the appropriate FE spaces

# Finite element scheme

The scheme

- semi-implicit
- produces one linear system per time step
- first order in time (may be generalized to the second order)
- unconditionally stable (stability estimate without CFL restriction) and 2nd order accurate, proved with assumptions:
  - $\inf_Q J \geq c_J > 0, \quad \sup_Q(\|\mathbf{F}\|_F + \|\mathbf{F}^{-1}\|_F) \leq C_F$
  - LBB-stable pairs (e.g. $P_2/P_1$)
  - $\Delta t$ is not large

A.Danilov, A.Lozovskiy, M.Olshanskii, Yu.Vassilevski. A finite element method for the Navier-Stokes equations in moving domain with application to hemodynamics of the left ventricle. *Russian J. Numer. Anal. Math. Modelling, 32, 2017*

A.Lozovskiy, M.Olshanskii, Yu.Vassilevski. A quasi-Lagrangian finite element method for the Navier-Stokes equations in a time-dependent domain. Comput.Methods Appl.Mech. Engrg.333,2018

# Stability estimate for the FE solution

Let $\partial\Omega(t) = \partial\Omega^{ns}(t)$ and $\boldsymbol{\xi}_t$ be given on $\partial\Omega^{ns}(t)$. Then there exists $\mathbf{v}_1 \in C^1(Q)^d$, $\mathbf{v}_1 = \boldsymbol{\xi}_t$, $\operatorname{div}(J\mathbf{F}^{-1}\mathbf{v}_1) = 0$ [Miyakawa1982]

and we can decompose the solution $\mathbf{v} = \mathbf{w} + \mathbf{v}_1$, $\mathbf{w} = 0$ on $\partial\Omega^{ns}$

Energy balance for $\mathbf{w}_h^k$ FE approximation of $\mathbf{w}^k$:

$$\underbrace{\frac{1}{2\Delta t}\left(\|J_k^{\frac{1}{2}}\mathbf{w}_h^k\|^2 - \|J_{k-1}^{\frac{1}{2}}\mathbf{w}_h^{k-1}\|^2\right)}_{\text{variation of kinetic energy}} \quad \underbrace{+2\nu\left\|J_k^{\frac{1}{2}}\mathbf{D}_k(\mathbf{w}_h^k)\right\|^2}_{\text{energy of viscous dissipation}} \quad \underbrace{+\frac{(\Delta t)}{2}\left\|J_{k-1}^{\frac{1}{2}}[\mathbf{w}_h]_t^k\right\|^2}_{O(\Delta t)\text{ dissipative term}}$$

$$\underbrace{+(J_k(\nabla\mathbf{v}_1^k\mathbf{F}_k^{-1})\mathbf{w}_h^k, \mathbf{w}_h^k)}_{\text{intensification due to b.c.}} \quad = \quad \underbrace{(\widetilde{\mathbf{f}}^k, \mathbf{w}_h^k)}_{\text{work of ext. forces}}$$

A.Danilov, A.Lozovskiy, M.Olshanskii, Yu.Vassilevski. A finite element method for the Navier-Stokes equations in moving domain with application to hemodynamics of the left ventricle. *Russian J. Numer. Anal. Math. Modelling, 32, 2017*

# Stability estimate for the FE solution

Stability estimate for $\mathbf{w}_h^n$ FE approximation of $\mathbf{w}^n$:

$C_1\|\nabla \mathbf{v}_1^k\| \leq \nu/2$:

$$\frac{1}{2}\|\mathbf{w}_h^n\|_n^2 + \nu \sum_{k=1}^{n} \Delta t \|\mathbf{D}_k(\mathbf{w}_h^k)\|_k^2 \leq \frac{1}{2}\|\mathbf{w}_0\|_0^2 + C \sum_{k=1}^{n} \Delta t \|\widetilde{\mathbf{f}}^k\|^2$$

$$\mathbf{D}_k(\mathbf{v}) := \tfrac{1}{2}(\nabla \mathbf{v} \mathbf{F}_k^{-1} + \mathbf{F}_k^{-T}(\nabla \mathbf{v})^T)$$

A.Danilov, A.Lozovskiy, M.Olshanskii, Yu.Vassilevski. A finite element method for the Navier-Stokes equations in moving domain with application to hemodynamics of the left ventricle. *Russian J. Numer. Anal. Math. Modelling, 32, 2017*

# Stability estimate for the FE solution

Stability estimate for $\mathbf{w}_h^n$ FE approximation of $\mathbf{w}^n$:

$C_1\|\nabla \mathbf{v}_1^k\| \leq \nu/2$:

$$\frac{1}{2}\|\mathbf{w}_h^n\|_n^2 + \nu \sum_{k=1}^{n} \Delta t \|\mathbf{D}_k(\mathbf{w}_h^k)\|_k^2 \leq \frac{1}{2}\|\mathbf{w}_0\|_0^2 + C \sum_{k=1}^{n} \Delta t \|\widetilde{\mathbf{f}}^k\|^2$$

$$\mathbf{D}_k(\mathbf{v}) := \tfrac{1}{2}(\nabla \mathbf{v} \mathbf{F}_k^{-1} + \mathbf{F}_k^{-T}(\nabla \mathbf{v})^T)$$

$C_1\|\nabla \mathbf{v}_1^k\| > \nu/2$:

$$\frac{1}{2}\|\mathbf{w}_h^n\|_n^2 + \nu \sum_{k=1}^{n} \Delta t \|\mathbf{D}_k(\mathbf{w}_h^k)\|_k^2 \leq e^{\frac{2C_2}{\alpha}T} \left( \frac{1}{2}\|\mathbf{w}_0\|_0^2 + C \sum_{k=1}^{n} \Delta t \|\widetilde{\mathbf{f}}^k\|^2 \right),$$

$$\text{if } (1 - 2C_2\Delta t) = \alpha > 0$$

A.Danilov, A.Lozovskiy, M.Olshanskii, Yu.Vassilevski. A finite element method for the Navier-Stokes equations in moving domain with application to hemodynamics of the left ventricle. *Russian J. Numer. Anal. Math. Modelling, 32, 2017*

# Convergence of the FE solution

Assume

1. LBB stable FE pair $P_{m+1}$-$P_m$;
2. $\Omega_0$ is a convex polyhedron;
3. $\mathbf{u}_{tt} \in L^\infty(\Omega_0)$, $\mathbf{u}(t) \in H^{m+\frac{5}{2}}(\Omega_0)$, $p(t) \in H^{m+1}(\Omega_0)$ for all $t \in [0, T]$;
4. $c\Delta t \geq h^{2m+4}$ with some $c$ independent of $h$, $\Delta t$;
5. either $\Delta t$ is small enough s.t. $\frac{1}{2} - \tilde{C}\Delta t > 0$ or $\nu \geq \tilde{C}\, C_K$

Then

$$\max_{1\leq k\leq N} \|\mathbf{e}^k\|_k^2 + 2\nu\Delta t \sum_{k=1}^{N} \|\mathbf{D}_k(\mathbf{e}^k)\|_k^2 \leq C\left(h^{2(m+1)} + (\Delta t)^2 + (\Delta t)^{-1} h^{2(m+2)}\right).$$

In particular, for Taylor-Hood pair, $m = 1$:

$$\max_{1\leq k\leq N} \|\mathbf{e}^k\|_k^2 + 2\nu\Delta t \sum_{k=1}^{N} \|\mathbf{D}_k(\mathbf{e}^k)\|_k^2 \leq C \max\{h^2; \Delta t\} \text{ if } h^2 \leq c\Delta t.$$

A.Lozovskiy, M.Olshanskii, Yu.Vassilevski. A quasi-Lagrangian finite element method for the Navier-Stokes equations in a time-dependent domain. Comput. Methods Appl. Mech. Engrg. 333, 2018

# 3D: left ventricle of a human heart

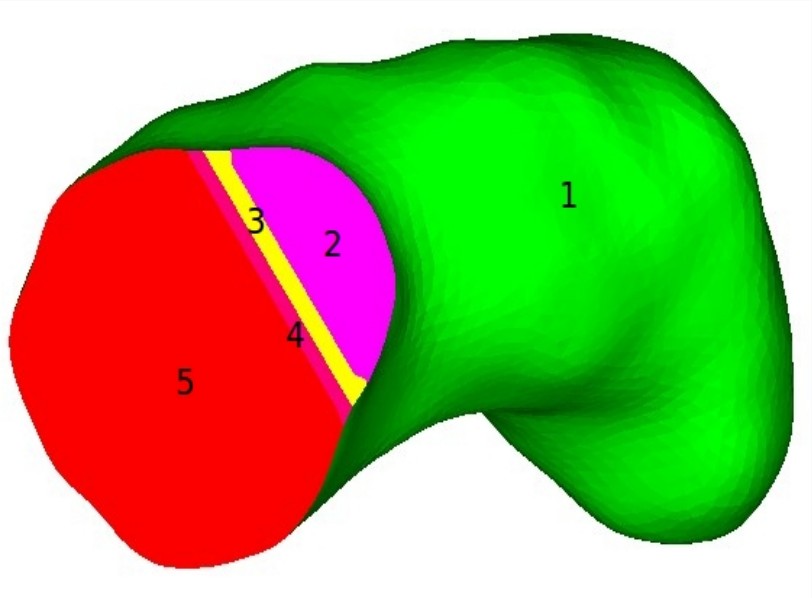


**Рис. 1:** Left ventricle

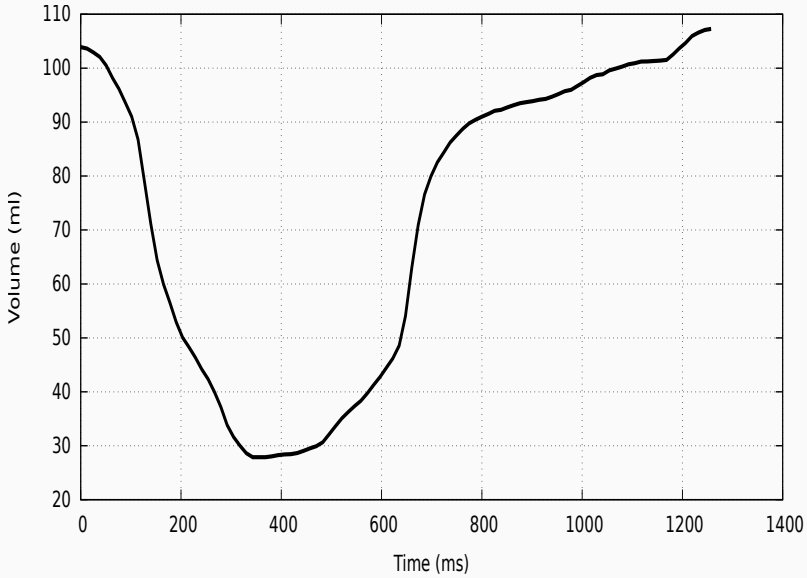


**Рис. 2:** Ventricle volume

The law of motion for the ventricle walls is known thanks to ceCT scans $\rightarrow$ 100 mesh files with time gap 0.0127 s $\rightarrow$ $\mathbf{u}$ given as input

- 2 - aortic valve (outflow)
- 5 - mitral valve (inflow)

# 3D: left ventricle of a human heart

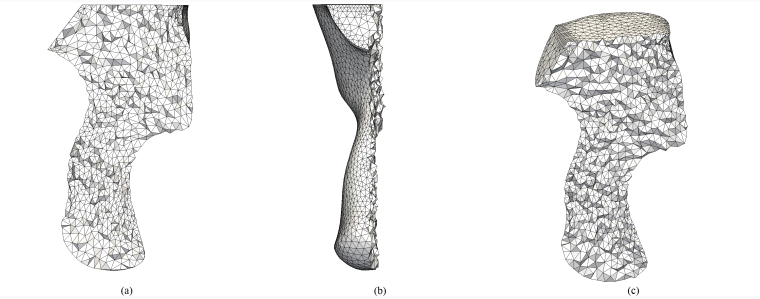


- Quasi-uniform mesh: 14033 vertices, 69257 elements, 88150 edges.
- Boundary conditions: Dirichlet $\mathbf{v} = \frac{\partial \mathbf{u}}{\partial t}$ except:
  - Do-nothing on aortal valve during systole
  - Do-nothing on mitral valve during diastole
- Time step 0.0127 s is too large! $\Longrightarrow$ refined to $\Delta t = 0.0127/20$ s $\Longrightarrow$ Cubic-splined $\mathbf{u}$.
- Blood parameters: $\rho_f = 10^3$ kg/m$^3$, $\mu_f = 4 \cdot 10^{-3}$ Pa ·s.

# 3D: left ventricle of a human heart

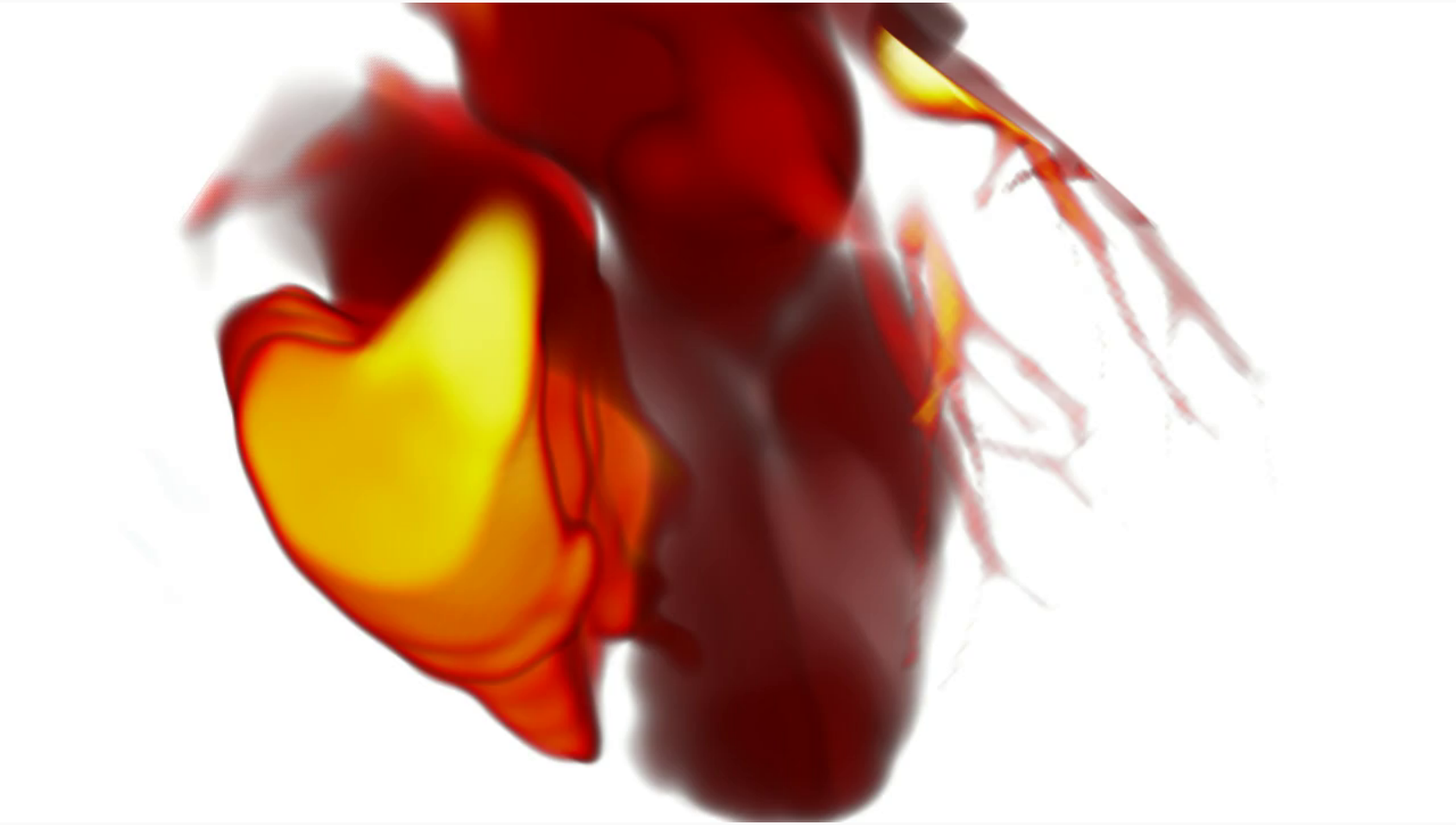

# Example 2

# Navier-Stokes equations for flows in rigid walls



- 1D hemodynamic simulations are low-cost and are appealing in clinical applications
- But they do not provide 3D fields
- 3D Navier-Stokes equations for incompressible flows in rigid walls are easier-to-solve than FSI, give 3D fields
- But they can not give correct averaged flow rates and pressures for a straight vessel
- However, in case of a bifurcation, 3D NS eq. can provide 3D fields and correct averaged flow rates and pressures within a multiscale framework

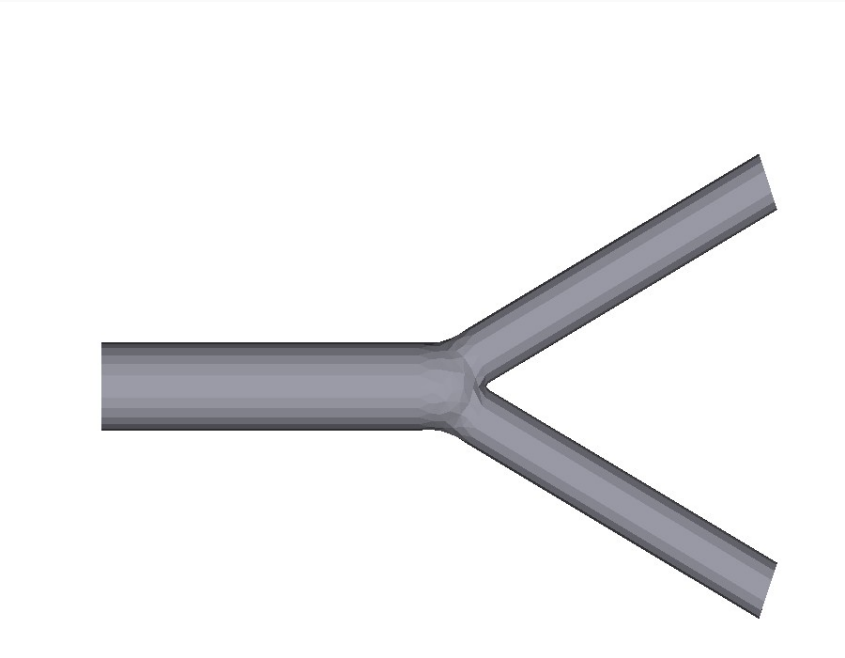

T.Dobroserdova, F.Liang, G.Panasenko, Yu.Vassilevski. Multiscale models of blood flow in the compliant aortic bifurcation *Applied Mathematics Letters 93C, 2019*

# Navier-Stokes equations in aortic bifurcation

- 3D Navier-Stokes equations for flow in rigid wall in bifurcation vicinity
- 1D hemodynamic equations (cross-area averaged flow in collapsible tubes)
- 0D lumped model (elastic sphere filled by fluid)

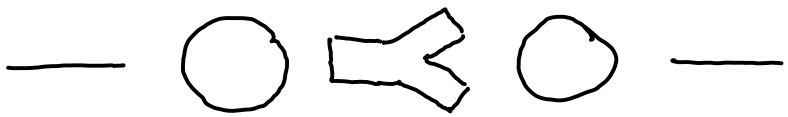

# Navier-Stokes equations in aortic bifurcation

Mass and momentum balance in each vessel

$$\begin{aligned} \partial S_k/\partial t + \partial(S_k u_k)/\partial x &= 0, \\ \partial u_k/\partial t + \partial\left(u_k^2/2 + p_k/\rho\right)/\partial x &= -\frac{8\pi\mu u_k}{S_k}, \end{aligned}$$

$\rho$ is the blood density (constant), $S_k(t,x)$ is the cross-section area, $u_k(t,x)$ is the linear velocity averaged over the cross-section, $p_k(S_k)$ is the blood pressure

# Navier-Stokes equations in aortic bifurcation

Elastic sphere with volume $V = V(t)$ filled with fluid is the 0D absorber

$$p_{0\mathrm{D}}(t) = p_{fluid} - p_{ext}$$

The kinematics of the sphere is:

$$I\frac{d^2V}{dt^2} + R_0\frac{dV}{dt} + \frac{V - V_0}{C} = p_{0\mathrm{D}}$$

# Navier-Stokes equations in aortic bifurcation

The conservation of mass:

$$\frac{dV}{dt} = Q_{1\mathrm{D}} - Q_{3\mathrm{D}},$$

$Q_{1\mathrm{D}} = S\overline{v}$, $Q_{3\mathrm{D}} = -\int_\Gamma \mathbf{v}\cdot\mathbf{n}ds$

Poiseuille law links the flow rate to the pressure drop:

$$\begin{aligned} \overline{p} - p_{0\mathrm{D}} &= R_{1\mathrm{D}0\mathrm{D}} Q_{1\mathrm{D}} \qquad \text{at } x = b, \\ p_{0\mathrm{D}} - p &= R_{0\mathrm{D}3\mathrm{D}} Q_{3\mathrm{D}} \qquad \text{on } \Gamma, \end{aligned}$$

where $R_{1\mathrm{D}0\mathrm{D}}$ and $R_{0\mathrm{D}3\mathrm{D}}$ are the resistance coefficients introducing additional dissipation in the cumulative energy balance of the complete 1D–0D–3D system

T.Dobroserdova, M.Olshanskii, S.Simakov. Multi-scale coupling of compliant and rigid walls blood flow models. Int.J.Num.Meth.Fluids, 82(12):799-817, 2016

# Navier-Stokes equations in aortic bifurcation

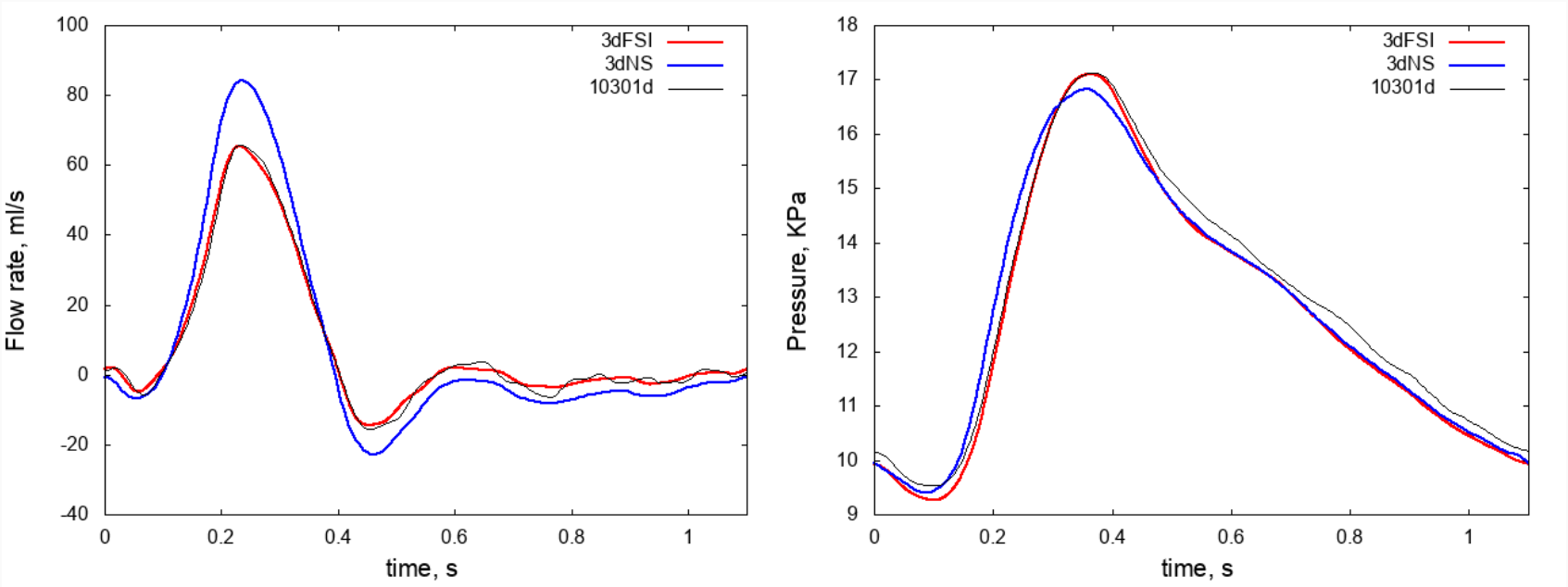


| Error in | flux | | pressure | |
|---|---|---|---|---|
| Method | avg% | max% | avg% | max% |
| 1dHem | 0.78 | 3.53 | 0.41 | 0.74 |
| 3dNS | 9.15 | 30.02 | 1.41 | 8.31 |
| 10301d | 1.15 | 4.49 | 2.02 | 3.48 |

T.Dobroserdova, F.Liang, G.Panasenko, Yu.Vassilevski. Multiscale models of blood flow in the compliant aortic bifurcation *Applied Mathematics Letters 93C, 2019*

# For details refer to

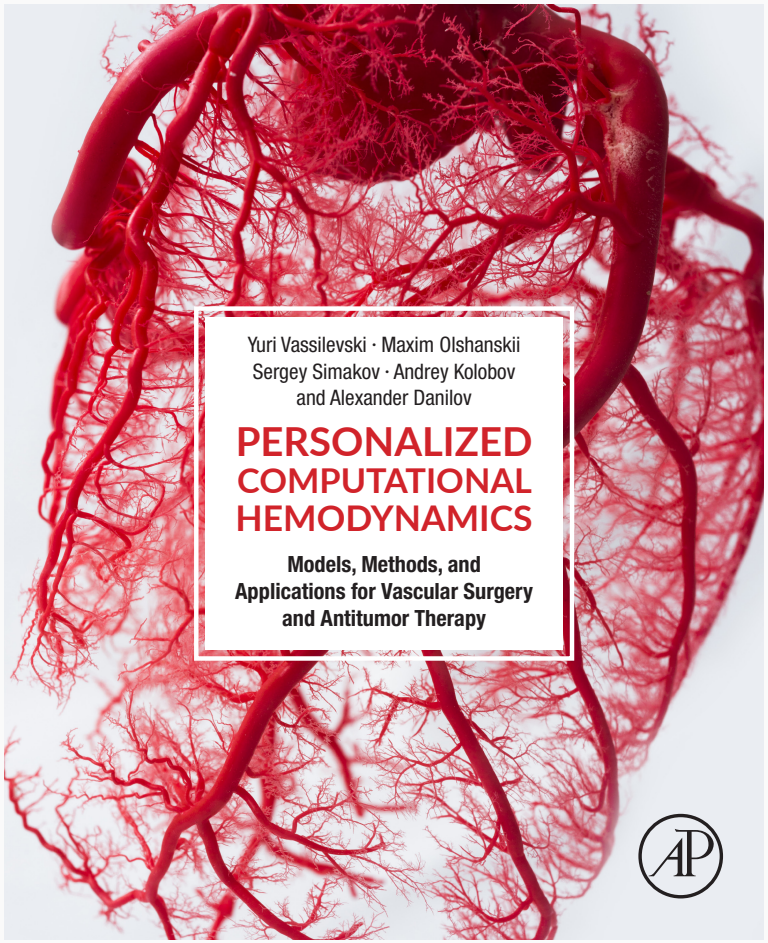


Y.Vassilevski, M.Olshanskii,
S.Simakov, A.Kolobov, A.Danilov

Personalized Computational Hemodynamics:
Models, Methods, and Applications for
Vascular Surgery and Antitumor Therapy

Academic Press 2020, ISBN: 9780128156537

# Example 3

# Patient-specific modeling of aortic valve closing

V.Salamatova, A.Danilov, A.Lyogkii, R.Pryamonosov

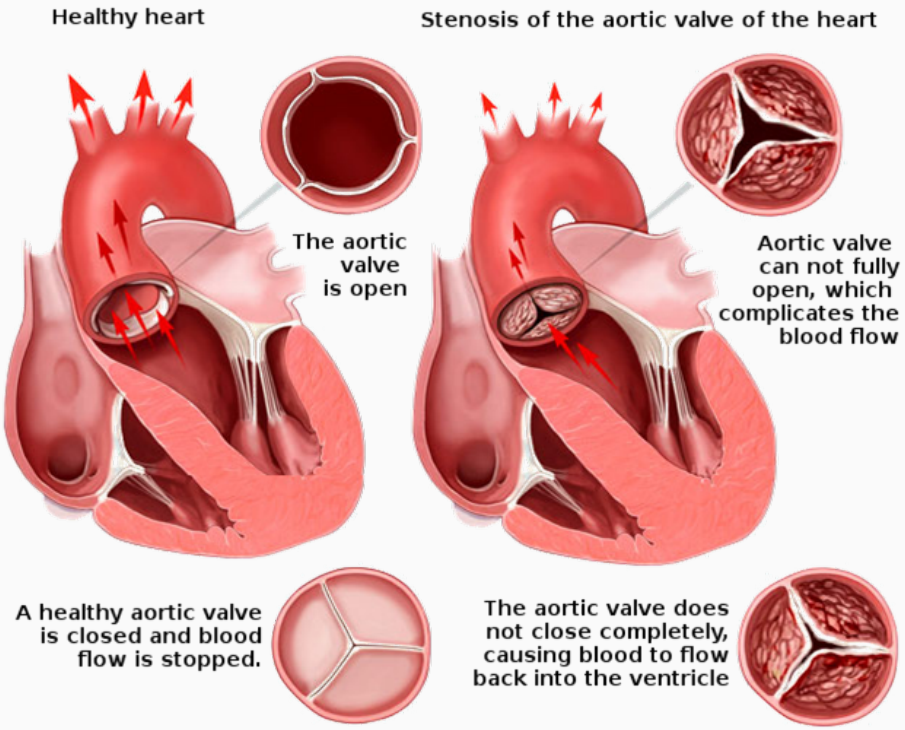


Aortic valve cusps replacement by leaflets cut from pericardium:

- no immune response
- efficient, low-cost
- all measurements and cuttings are made during operation

# Patient-specific modeling of aortic valve closing

Objectives of modeling:

- degree of regurgitation
- height of coaptation

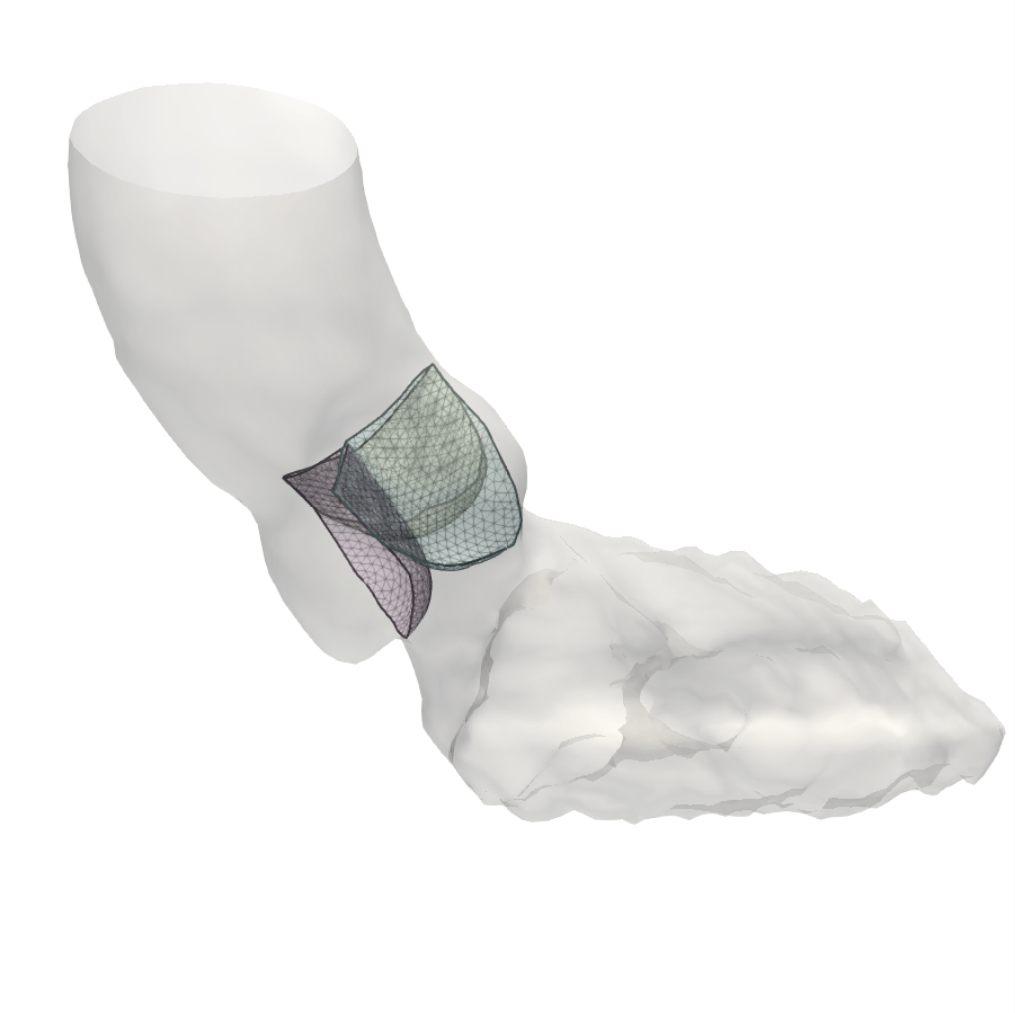

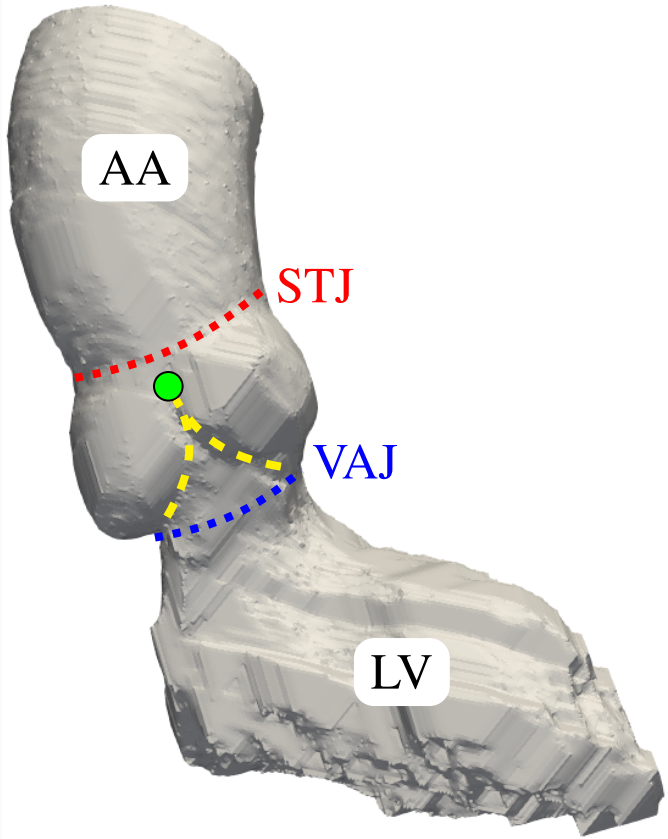

# Patient-specific modeling of aortic valve closing

The mass-spring model (MSM) computes leaflet deformation under diastolic pressure:

- leaflet is an oriented triangulated surface
- each edge is a spring with given stiffness
- each node has a point mass at which forces due to springs and pressure are applied

$$\mathbf{F}_{ij} = k_{ij}(\|\mathbf{r}_j - \mathbf{r}_i\| - L_{ij})\frac{\mathbf{r}_j - \mathbf{r}_i}{\|\mathbf{r}_j - \mathbf{r}_i\|}$$

$$k_{ij} = \frac{E(\varepsilon, \alpha_0)HA_{ij}}{L_{ij}^2}$$

- we search static equilibrium

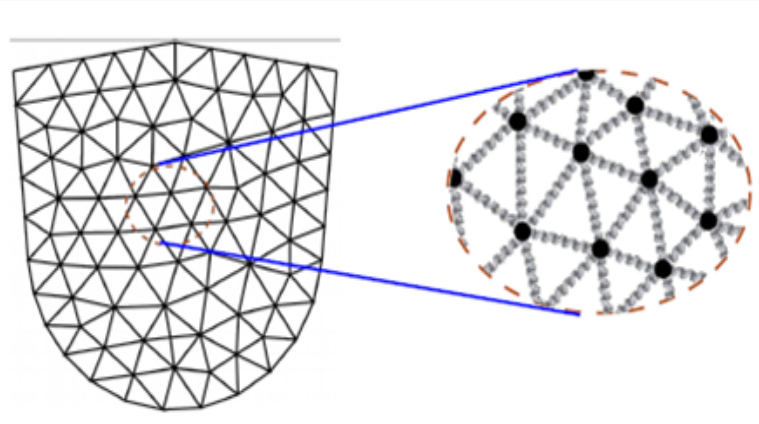

A.VanGelder. Approximate simulation of elastic membranes by triangulated spring meshes

J. Graph. Tools. 1998

# Patient-specific modeling of aortic valve closing

| Size | | Isotropic | ↑ | → | ↗ |
|---|---|---|---|---|---|
| 22 | $h$ | 14.3 | 14.3 | 14.2 | 14.2 |
| 26 | $h$ | 16.4 | 16.2 | 16.3 | 16.6 |
| 28 | $h$ | 16.8 | 16.2 | 17.0 | 16.9 |
| 22 | $h_c$ | 0 | 0 | 0 | 0 |
| 26 | $h_c$ | 11.6 | 10 | 10.1 | 12.2 |
| 28 | $h_c$ | 11.9 | 13.4 | 12.7 | 13.2 |

Coaptation height (mm) for 3 leaflet sizes (mm) and anisotropy directions

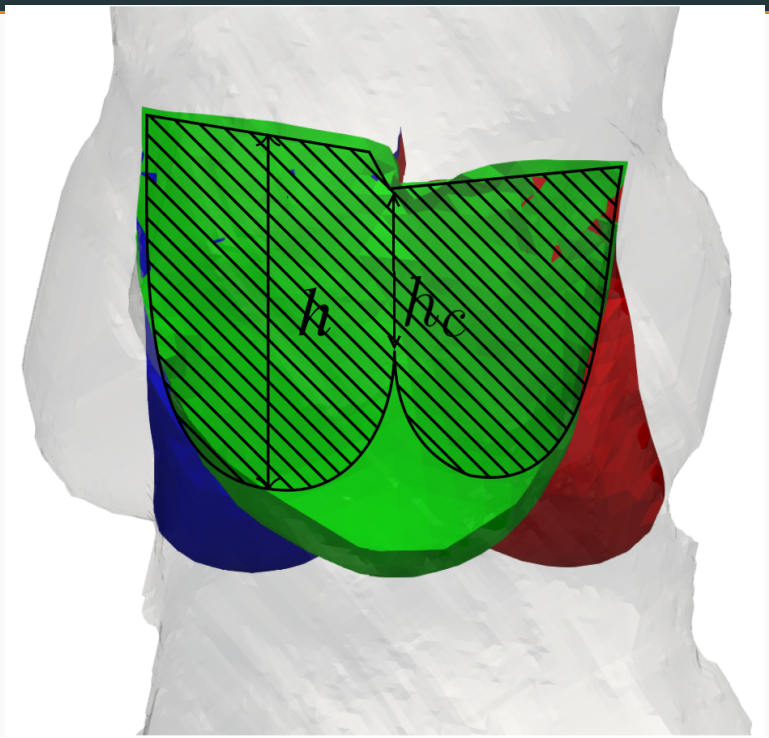


Hyperelastic nodal force method (V.Salamatova) allows us to simulate coaptation of cusps from hyperelastic materials

V.Salamatova, A.Liogky, P.Karavaikin et al. Numerical assessment of coaptation for auto-pericardium based aortic valve cusps. *Russian J. Numer. Anal. Math. Modelling, 34, 2019*

# Patient-specific modeling of aortic valve closing

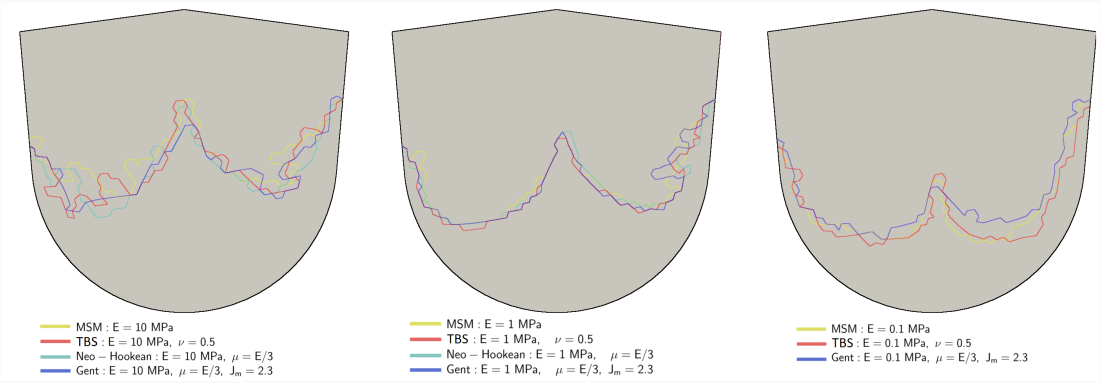


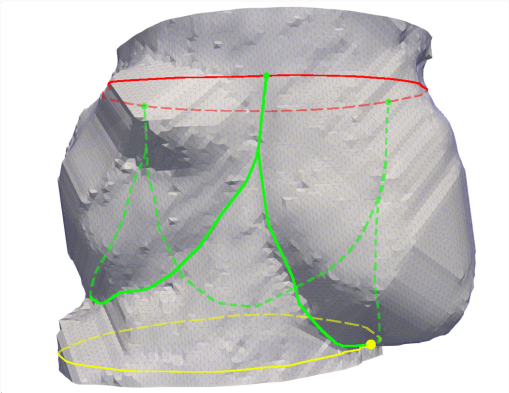

Coaptation profiles for different elasticity models and elastic modulii (upper row), suturing paths and commissures on the aorta (bottom).

V.Salamatova, A.Liogky, P.Karavaikin et al. Numerical assessment of coaptation for auto-pericardium based aortic valve cusps. *Russian J. Numer. Anal. Math. Modelling, 34, 2019*

Thank you for your attention!